Urologia
Internationalis

Urol Int, DOI: 10.1159/uin/aewag010
Received: March 22, 2026
Accepted: July 12, 2026
Published online: August 19, 2026

MRI-Based Prediction of Positive Surgical Margins in Radical Prostatectomy: Insights from Clinical and Imaging Parameters

Niessen C., Gromes Y., Engelmann S.U., Haas M., Kälble S., Bründl J., Stroszczynski C., Burger M., Weber F., Pickl C.

ISSN: 0042-1138 (Print), eISSN: 1423-0399 (Online)
https://www.karger.com/UIN
Urologia Internationalis

MRI-Based Prediction of Positive Surgical Margins in Radical Prostatectomy: Insights from Clinical and Imaging Parameters

Journal: Urologia Internationalis

UIN-2026-3-18/R1 RESUBMISSION

Manuscript Type: Research Article

Keywords: Prostate cancer, multiparametric MRI, positive surgical margins, robot-assisted radical prostatectomy, extraprostatic extension

Authors:
Christoph Niessen, PD Dr. med. (Corresponding author)
Yannick Gromes, Mr (Co-author)
Simon Udo Engelmann, Dr. med. (Co-author)
Maximilian Haas, Dr. (Co-author)
Sebastian Kälble, Dr. (Co-author)
Johannes Bründl, Prof. (Co-author)
Christian Stroszczynski, Prof. (Co-author)
Maximilian Burger, Prof. (Co-author)
Florian Weber, PD Dr. med. (Co-author)
Christoph Pickl, Dr. med. (Co-author)

MRI-Based Prediction of Positive Surgical Margins in Radical Prostatectomy: Insights from Clinical and Imaging Parameters

Christoph Niessen[1#], Yannick Gromes[2], Simon Udo Engelmann[3], Maximilian Haas[3], Sebastian Kälble[3], Johannes Bründl[3], Christian Stroszczynski[2], Maximilian Burger[3], Florian Weber[4], Christoph Pickl[3]

[1] Institute for Radiology, Caritas Hospital St. Josef, Regensburg, Germany
[2] Institute for Radiology, University Hospital Regensburg, Regensburg, Germany
[3] Department of Urology, University Hospital Regensburg, Regensburg, Germany
[4] Institute for Pathology, University of Regensburg, Regensburg, Germany
[#] Corresponding author

Short title: MRI-Based Prediction of Positive Surgical Margins in Radical Prostatectomy

Corresponding author

Christoph Niessen

E-mail address: cniessen@csj.de

Keywords:

Prostate cancer, multiparametric MRI, positive surgical margins, robot-assisted radical prostatectomy, extraprostatic extension

Abstract:

Introduction:

Positive surgical margins (PSM) after radical prostatectomy are associated with adverse oncological outcomes. Preoperative identification of patients at risk may improve surgical decision-making. The objective of this study was to evaluate clinical and MRI-derived predictors of PSM and to explore their potential value for preoperative risk assessment in patients undergoing robot-assisted radical prostatectomy (RARP).

Methods:

This retrospective, single-center study comprised 134 patients with localized prostate cancer who underwent preoperative multiparametric MRI (mpMRI) and RARP between July 2022 and April 2024. Clinical, histopathological, and MRI-derived parameters were analyzed using univariate and multivariate logistic regression. Odds ratios (ORs), 95% confidence intervals (CIs), and p-values were reported. Model performance was evaluated using receiver operating characteristic (ROC) curve analysis.

Results:

PSMs were present in 20.1% (27/134) of patients. In multivariate analysis, the strongest independent predictors of PSM were suspicion of extraprostatic extension (EPE) on MRI (OR 12.62, 95% CI 3.24–49.15; $p < 0.001$), urethral involvement (distance < 2 mm) (OR 8.88, 95% CI 1.76–44.73; $p = 0.008$), and capsular contact length >12 mm (OR 8.84, 95% CI 2.44–32.03; $p < 0.001$). The exploratory model achieved excellent apparent discrimination (AUC 0.911). Infiltration of the perineural sheath was observed in 96% of R1 compared to 70% of R0 patients ($p = 0.01$). Nerve-sparing surgery was not significantly associated with a different rate of PSM ($p = 0.385$).

Conclusion:

Several MRI-derived parameters, including capsular contact length, MRI-suspected extraprostatic extension, and urethral proximity, were associated with an increased likelihood of positive surgical margins. Incorporating these metrics alongside clinical factors may improve risk stratification. However, prospective studies with external validation are required before routine clinical implementation.

Introduction

Prostate cancer is the most prevalent malignancy diagnosed in men worldwide and a leading cause of cancer-related mortality (1–3). Radical prostatectomy is one of the primary treatment options for localized disease, aiming for complete resection of cancerous tissue (4). Achieving negative surgical margins is critical to lower the risk of biochemical recurrence, disease progression, and the need for adjuvant therapies (5). Positive surgical margins (PSM), have been consistently associated with poorer oncologic outcomes and represent a significant challenge in prostate cancer surgery (6,7).

Recent advances in multiparametric MRI (mpMRI) have enhanced preoperative planning and staging in prostate cancer by enabling detailed visualization of tumor characteristics, such as extraprostatic extension (EPE), lesion volume, and capsular contact. The PI-RADS (Prostate Imaging Reporting and Data System) scoring system is the standardized method for assessing prostate lesions. Lesions with a PI-RADS score of 4 and 5 are more likely to be cancerous and are often linked to adverse pathological outcomes (8,9). Preoperative mpMRI of the prostate provides valuable information on tumor aggressiveness and aids in evaluating EPE (10,11).

Certain MRI characteristics, including lesion diameter, capsular contact, and apical tumor involvement, have been identified as important predictors of PSM. Quentin et al. emphasized that larger lesion diameters and extended capsular contact lengths are associated with higher PSM risk (12). Similarly, Veerman et al. reported that apical tumor involvement, a challenging area to completely resect, significantly increases the probability of PSM and biochemical recurrence (13). These findings underscore the potential of using MRI-derived anatomical markers to predict surgical margin status, thereby supporting more tailored preoperative strategies.

Despite these advances, current literature reveals variability in how MRI features are utilized to predict PSM. Xu et al. attempted to develop a MRI-based grading system for PSM risk. However, a comprehensive and standardized predictive tool that integrates clinical and imaging features has yet to be established (14). Further research is necessary to validate which MRI and clinical factors most effectively predict PSM.
This study aims to fill this gap by evaluating specific clinical and MRI-derived factors to assess their association with PSM in patients undergoing robot-assisted laparoscopic-radical prostatectomy (RARP).

Methods

Patient selection

A total of 857 patients underwent RARP for localized prostate cancer at St. Josef Hospital in Regensburg between July 2022 and April 2024. Indications for RARP were determined by a certified tumor board conference, ensuring consistent, evidence-based decision-making aligned with institutional standards. Inclusion criteria required an in-house preoperative mpMRI with at least one MRI-visible lesion (PI-RADS $\geq$ 3) followed by in-house ultrasound-guided fusion biopsy with histologically confirmed prostate cancer, comprehensive clinical and imaging data, and documented pathological margin status post-surgery. Patients were excluded if they had received neoadjuvant therapy or if the preoperative MRI examinations were deemed non-evaluable due to insufficient image quality or incomplete sequences. This retrospective study was reviewed and approved by the Ethics Committee of the University of Regensburg through a simplified review procedure (reference number: 25-4399-104). Written informed consent for the use of clinical and imaging data for research purposes was obtained from all patients.

Preoperative imaging

All preoperative mpMRI examinations were performed using a Siemens Vida 3T scanner with a standardized protocol. Imaging sequences included pre-contrast axial T1-weighted turbo spin echo (TSE) imaging of the pelvis, T2-weighted TSE sequences in axial, coronal, and sagittal planes focused on the prostate, axial diffusion-weighted imaging (DWI) with b-values of 0, 800, and 1600 and a calculated b-value of 2000 and ADC map calculation, and dynamic contrast-enhanced (DCE) imaging using a gadolinium-based contrast agent at a dosage of 0.1 mmol/kg, injected at a rate of 2 mL/s. DCE imaging consisted of 30 series of T1-weighted vibe-twist sequences, followed by post-contrast coronal and axial T1-weighted TSE sequences of the pelvis. The slice thickness was set to 3 mm for all sequences focusing on the prostate and 5 mm for sequences covering the whole pelvis. Additional acquisition parameters included a field of view of 220 mm and repetition and echo times consistent with institutional standards.

MRI scans were reviewed by two board-certified radiologists with over ten years of experience in consensus reading, blinded to clinical information, who assigned PI-RADS scores (v2.1) and assessed lesion characteristics. Lesion diameter was measured along the longest dimension. Bilateral tumor presence was assessed based on MRI and biopsy findings. Capsular contact was measured on T2-weighted images as the extent of contiguous contact between the lesion and the prostatic capsule. EPE was assessed based on findings from T2-weighted images or DCE imaging, depending on which sequence provided clearer delineation of potential capsule breach using a 5-point Likert scale based on established MRI criteria, with scores ranging from 1 (definitely absent) to 5 (definitely present). For statistical analysis, Likert scores ≥4 were considered positive for EPE. Urethral involvement was defined as a minimum distance of less than 2 mm between the PI-RADS lesion and the urethra measured on axial T2-weighted images. Lesion density was defined as the sum of the maximal diameters of all MRI-detected lesions divided by the prostate volume, yielding a prostate size–adjusted surrogate of intraprostatic lesion burden.

<u>Pre-operative biopsy and pathological analysis</u>

An MRI–ultrasound fusion biopsy of the prostate was performed using a transrectal ultrasound (TRUS) system equipped with software-based image fusion (FusionVu, Philips Healthcare). Real-time TRUS images were fused with pre-acquired multiparametric MRI datasets to enable targeted sampling of MRI-visible lesions. For each lesion classified as PI-RADS category 3 or higher, two targeted biopsy cores were obtained. Targeted biopsies were complemented by systematic 12-core biopsy sampling according to institutional standards to ensure comprehensive histopathological assessment.

<u>Radical prostatectomy and pathological analysis</u>

All RARPs were performed using a robotic surgical platform (da Vinci Xi, Intuitive Surgical, Sunnyvale, California, USA) by a consistent surgical team. The procedure involved nerve-sparing techniques where oncologically appropriate. The prostate was removed en bloc, and vesicourethral anastomosis was completed.

Radical prostatectomy specimens were fixed in formalin and processed according to standard uropathological standards. Surgical margins were inked before sectioning, and the specimens were completely embedded and examined by experienced genitourinary pathologists. Histopathological evaluation included assessment of ISUP grade group, extraprostatic extension, seminal vesicle invasion, perineural invasion, and surgical margin status with PSM defined as the presence of tumor cells at the inked margin of the resected specimen. ISUP grading was conducted according to the 2014 International Society of Urological Pathology guidelines.

<u>Statistical analysis</u>

For statistical analysis, univariate associations with PSM were evaluated using Mann-Whitney U tests for continuous variables and Chi Square or Fisher's exact tests for categorical variables. As the aim of the model was preoperative risk assessment, only preoperatively available clinical, histopathological and MRI-derived variables with $p < 0.05$ in univariate analysis were considered for inclusion into a multivariate logistic regression model. Odds ratios (ORs) and 95% confidence intervals (CIs) were calculated. Missing data were excluded pairwise, and analyses were conducted using SPSS version 27 (IBM Corp., Armonk, NY, USA). Model performance was evaluated using a receiver operating characteristic (ROC) curve, with the area under the curve (AUC) representing discriminative power.

Results

During the study period, 857 patients underwent robot-assisted radical prostatectomy at our institution. After application of the predefined inclusion and exclusion criteria, 723 patients were excluded. The reasons for exclusion were the absence of an in-house preoperative multiparametric MRI (n = 589), external MRI–ultrasound fusion biopsy performed outside the institution (n = 127), non-diagnostic MRI due to severe artifacts caused by total hip replacement (n = 2), and neoadjuvant androgen deprivation therapy (n = 5). The final study cohort therefore consisted of 134 patients with 202 MRI-visible lesions.

<u>Clinical Parameters and Serum PSA Levels</u>

PSA levels were significantly higher in the R1 group (32.5 ± 78.9 ng/ml) than in the R0 group (8.9 ± 6.7 ng/ml; $p < 0.001$). PSA density was also significantly higher in R1 patients (0.33 ± 0.54 vs 0.11 ± 0.09 ng/ml²; $p < 0.001$), with PSA density >0.15 observed in 59% of R1 vs 24% of R0 cases ($p < 0.001$) (Table 1A). In logistic regression, PSA density yielded an OR of 6.61 (95% CI: 1.92–23.10; $p < 0.001$), and PSA density >0.15 had an OR of 4.53 (95% CI: 1.87–10.99; $p < 0.001$). No significant differences were observed for age, BMI, or prostate volume.

<u>Histopathological Characteristics</u>

The R1 group had a higher percentage of positive specimen tissue (43.7 ± 22.3%) compared to the R0 group (34.7 ± 20.0%; $p = 0.029$), with an OR of 1.02 (95% CI: 1.00–1.04; $p = 0.048$). Perineural invasion occurred in 96% of R1 vs. 70% of R0 patients ($p < 0.001$), which corresponded to an OR of 10.61 (95% CI: 1.38–81.60; $p = 0.023$). Pathological EPE was more prevalent in R1 cases (48% vs 28%; $p = 0.037$), with an OR of 2.38 (95% CI: 1.04–

5.66; $p = 0.049$). Seminal vesicle infiltration was observed in 15% of R1 vs 4% of R0 cases ($p = 0.046$), with an OR of 4.48 (95% CI: 1.04–19.24; $p = 0.044$) (Table 1B). Neither biopsy ISUP grade group nor prostatectomy specimen ISUP grade group differed significantly between patients with negative and positive surgical margins (Table 1A). MRI-derived characteristics according to surgical margin status are summarized in Table 2.

Surgical Parameters

The duration of RARP was significantly longer in the R1 group (3.14 ± 0.57 h) compared to the R0 group (2.87 ± 0.66 h; $p = 0.046$), with an OR of 1.93 (95% CI: 0.98–3.78) (Table 1A and Table 3). The time interval between MRI and surgery was shorter in R1 cases (114.2 ± 64.1 vs 136.0 ± 69.5 days), without being statistically significant ($p = 0.158$). Nerve-sparing surgery was performed in 52% of the R1 and 62% of the R0 patients ($p = 0.385$), with no significant association with PSM status (Table 1A).

MRI-Derived Characteristics

The maximum PI-RADS lesion diameter was larger in the R1 group (24.4 ± 16.8 mm) than in the R0 group (16.6 ± 8.1 mm; $p = 0.027$), corresponding to an OR of 1.06 (95% CI: 1.02–1.11; $p = 0.04$). Lesion density was significantly higher in R1 patients (0.35 ± 0.28 vs 0.22 ± 0.15 mm/cm^3; $p = 0.024$; OR = 19.05, 95% CI: 2.26–160.58; $p = 0.007$). Capsular contact was more common in R1 cases (93% vs 65%; $p = 0.004$), yielding an OR of 6.88 (95% CI: 1.55–30.66; $p = 0.011$). Contact length >12 mm was noted in 63% of R1 vs 16% of R0 patients ($p < 0.001$), with an OR of 9.00 (95% CI: 3.53–22.98; $p < 0.001$). Suspicion of EPE on MRI (Figure 1) was present in 59% of R1 vs 7% of R0 patients ($p < 0.001$), associated with an OR of 21.04 (95% CI: 7.27–60.88; $p < 0.001$). Urethral involvement <2 mm (Figure 2) was more frequent in the R1 group (41% vs 9%; $p < 0.001$), with an OR of 6.67 (95% CI: 2.44–18.25; $p < 0.001$). MRI-detected seminal vesicle infiltration ($p = 0.046$; OR = 4.48, 95% CI: 1.04–19.24) and hyperperfusion ($p < 0.001$; OR = 5.47, 95% CI: 2.29–13.08) were also more common in R1 patients. Apical involvement did not differ significantly between both groups.

Overall, 202 MRI-visible lesions were identified in the study cohort, including 162 lesions in patients with negative surgical margins and 40 lesions in patients with positive surgical margins. Lesions from patients with PSM exhibited significantly greater capsular contact length (13.2 ± 10.8 mm vs 5.5 ± 5.8 mm; $p < 0.001$), larger lesion volume (2.12 ± 3.74 vs 0.54 ± 0.68 cm^3; $p = 0.014$), higher PI-RADS scores (4.4 ± 0.5 vs 4.1 ± 0.5; $p = 0.005$), and shorter distances to the urethra (7.3 ± 6.5 vs 9.3 ± 5.4 mm; $p = 0.020$). Apical tumor location did not differ significantly ($p = 0.720$) (Table 1B and 2).

Multivariate Analysis

In multivariate analysis, suspicion of EPE (OR = 12.62, 95% CI: 3.24–49.15; $p < 0.001$), urethral involvement <2 mm (OR = 8.88, 95% CI: 1.76–44.73; $p = 0.008$), and capsular contact length >12 mm (OR = 8.84, 95% CI: 2.44–32.03; $p < 0.001$) in preoperative MRI remained strong independent predictors for PSM. PSA density >0.15 showed a nonsignificant trend toward association (OR = 3.06, 95% CI: 0.87–10.74; $p = 0.081$), while lesion density and seminal vesicle infiltration were not significantly associated with PSM. The final model demonstrated excellent discrimination (AUC = 0.911).

Discussion

In this retrospective single-center study, we examined the correlation between preoperative mpMRI-derived parameters and positive surgical margins in patients undergoing robot-assisted radical prostatectomy. The results align with prior research indicating a significant association between MRI-derived metrics - particularly extraprostatic extension, urethral involvement, and capsular contact - and the likelihood of positive surgical margins.

MRI-Derived Predictors

Consistent with previous studies, MRI-suspected extraprostatic extension, urethral proximity, and extensive capsular contact were associated with positive surgical margins (15,16). These findings support the concept that increased tumor extent and prolonged capsular contact may reflect a greater likelihood of extraprostatic spread (Figure 3 and 4), thereby increasing the risk of incomplete resection (17,18). However, in contrast to prior reports linking ADC values to margin status, no significant association was observed in our cohort (19).

Apical Involvement, Perineural Invasion and Surgical Technique

Apical involvement has been traditionally regarded as a critical risk factor for PSM. Yao et al. found that tumors involving the apex significantly increased PSM rates, presumably due to the anatomic complexity of achieving a clear resection margin in this region (20). In our study, however, we did not observe a significant association between apical involvement and margin status ($p = 0.484$). This discrepancy could be due to the advantages of using an interdisciplinary approach to preoperative MRI where radiologists and surgeons jointly assess tumor location—and the technical advantages of RARP, which can facilitate more precise apical dissection (Figure 5).

We also found no significant difference in PSM rates between nerve-sparing and non–nerve-sparing procedures (p= 0.385). While some authors suggest that nerve-sparing could increase margin positivity, especially in the posterolateral region, our data indicate that careful preoperative imaging assessment may assist in identifying patients for whom nerve-sparing surgery can be performed without an increased risk of margin positivity (21). Posterolateral PSMs are recognized as the second-most prevalent site of positive margins in prostatectomy specimens and have been associated with an increased risk of local recurrence (22). Perineural invasion, which is more frequently observed posterolaterally, may facilitate tumor spread beyond the prostatic capsule and thereby increase the risk of residual tumor especially when a nerve-sparing approach is employed (23,24). In our cohort, perineural invasion was strongly associated with PSMs ($p < 0.001$), underscoring its pathological relevance and the importance of meticulous surgical technique in affected regions.

<u>Seminal Vesicle Invasion and PSM</u>

Consistent with prior research, we observed a significantly higher prevalence of seminal vesicle invasion among patients with PSMs in univariable analysis ($p = 0.046$) (7). However, this association did not persist after multivariable adjustment indicating that seminal vesicle invasion itself may not constitute an independent determinant of margin positivity. Instead, its apparent relationship with PSMs may reflect its role as a surrogate marker of advanced tumor extent (Figure 6).

<u>Surgical Factors</u>

Interestingly, our data suggests that surgery duration might be associated with an increased risk of PSM. Longer procedures may indicate heightened surgical complexity or challenging tumor characteristics, potentially making it more difficult to achieve clear margins. Further investigation is warranted to clarify whether this factor simply reflects case difficulty or if targeted interventions - such as augmented intraoperative imaging or frozen-section analysis - could mitigate prolonged surgery times and reduce residual disease.

<u>Clinical Implications and Future Directions</u>

Taken together, these findings highlight the potential value of a thorough mpMRI evaluation in the preoperative setting. MRI-suspected extraprostatic extension, urethral proximity, and extended capsular contact may help identify patients at increased risk of PSM and may contribute to preoperative risk stratification. Our multivariate logistic regression model, which included these MRI parameters and key clinical factors, achieved good discriminatory performance (AUC = 0.911). However, given the limited number of events and the absence of an independent validation cohort, these results should be regarded as exploratory and hypothesis-generating rather than as a definitive clinical risk calculator. Although these findings suggest a potential role of MRI-derived parameters in surgical planning, prospective multicenter studies with external validation are required before routine clinical implementation.

<u>Limitations</u>

This study has several limitations. First, its retrospective single-center design may limit generalizability and introduce selection bias. Although a large number of patients underwent robot-assisted radical prostatectomy during the study period, only a subset met the strict inclusion criteria, primarily due to the requirement for in-house multiparametric MRI, MRI–ultrasound fusion biopsy, and complete pathological data. In addition, only patients with at least one MRI-visible lesion were included; therefore, the findings should not be extrapolated to patients without MRI-visible disease.

Second, the relatively small number of positive surgical margin events limits the statistical power of multivariable analyses. Consequently, the multivariable model should be interpreted as exploratory and hypothesis-generating rather than definitive. Although strong associations were observed for several MRI-derived parameters, the possibility of model overfitting cannot be excluded.

Third, no independent external validation cohort was available. Therefore, the predictive performance reported in this study may not fully translate to other institutions with different patient populations, imaging protocols, pathological processing, and surgical techniques. Prospective, multicenter studies with external validation are warranted to confirm the predictive value of MRI-derived parameters for positive surgical margins before clinical implementation.

Nevertheless, in contrast to several previous studies investigating MRI-based parameters to predict PSM, the standardized imaging and surgical workflow represents a methodological strength of the present cohort. All patients underwent mpMRI on the same 3-Tesla scanner using standardized sequences and consistent imaging protocols, and surgical procedures were performed by a consistent surgical team. This homogeneity may reduce variability related to imaging acquisition and operative technique, although it does not replace the need for external validation.

Conclusion

In this retrospective single-center study, MRI-derived parameters - specifically MRI-suspected extraprostatic extension, capsular contact length, and urethral proximity - were associated with an increased risk of positive surgical margins following robot-assisted radical prostatectomy. These results indicate that comprehensive preoperative mpMRI assessment may contribute to surgical planning and risk stratification, especially in anatomically challenging regions. However, due to the exploratory nature of the present analysis, prospective multicenter validation is required before these findings can be integrated into standard clinical decision-making.

Statement of Ethics

Study approval statement: This study was conducted in accordance with the Declaration of Helsinki and approved by the Ethics Committee of the University of Regensburg (reference number: 25-4399-104).

Consent to participate statement: Informed consent was waived due to the retrospective nature of the study and anonymized data analysis. Written consent was obtained for the publication of images of individual participants. This was done as part of the informed consent process for the MRI examination.

Conflicts of Interest Statement

The authors declare that they have no competing interests. Maximilian Burger was a member of the journal's Editorial Board at the time of submission.

Funding Sources

This research received no external funding.

Author Contributions

All authors contributed to the study conception and design. Material preparation, data collection and analysis were performed by YG, CN, CP, SUE, SK, MH, JB and FW. The first draft of the manuscript was written by CN and CP and all authors commented on previous versions of the manuscript. CS and MB supervised the research. All authors approved the final manuscript and consent for submission.

Data Availability Statement

Datasets generated or analyzed in this study are not publicly available due to data protection regulations but are available from the corresponding author on reasonable request.

References

1. Bergengren O, Pekala KR, Matsoukas K, Fainberg J, Mungovan SF, Bratt O, u. a. 2022 Update on Prostate Cancer Epidemiology and Risk Factors—A Systematic Review. Eur Urol. August 2023;84(2):191–206.
2. Siegel RL, Kratzer TB, Giaquinto AN, Sung H, Jemal A. Cancer statistics, 2025. CA Cancer J Clin. Januar 2025;75(1):10–45.
3. Rawla P. Epidemiology of Prostate Cancer. World J Oncol. 2019;10(2):63–89.
4. Cornford P, Van Den Bergh RCN, Briers E, Van Den Broeck T, Brunckhorst O, Darraugh J, u. a. EAU-EANM-ESTRO-ESUR-ISUP-SIOG Guidelines on Prostate Cancer—2024 Update. Part I: Screening, Diagnosis, and Local Treatment with Curative Intent. Eur Urol. August 2024;86(2):148–63.
5. Zhang L, Wu B, Zha Z, Zhao H, Jiang Y, Yuan J. Positive surgical margin is associated with biochemical recurrence risk following radical prostatectomy: a meta-analysis from high-quality retrospective cohort studies. World J Surg Oncol. Dezember 2018;16(1):124.
6. Meeks JJ, Eastham JA. Radical prostatectomy: Positive surgical margins matter. Urol Oncol Semin Orig Investig. Oktober 2013;31(7):974–9.
7. Zhang L, Zhao H, Wu B, Zha Z, Yuan J, Feng Y. Predictive Factors for Positive Surgical Margins in Patients With Prostate Cancer After Radical Prostatectomy: A Systematic Review and Meta-Analysis. Front Oncol. 8. Februar 2021;10:539592.
8. Turkbey B, Rosenkrantz AB, Haider MA, Padhani AR, Villeirs G, Macura KJ, u. a. Prostate Imaging Reporting and Data System Version 2.1: 2019 Update of Prostate Imaging Reporting and Data System Version 2. Eur Urol. September 2019;76(3):340–51.
9. Woo S, Suh CH, Kim SY, Cho JY, Kim SH. Diagnostic Performance of Prostate Imaging Reporting and Data System Version 2 for Detection of Prostate Cancer: A Systematic Review and Diagnostic Meta-analysis. Eur Urol. August 2017;72(2):177–88.
10. Jäderling F, Akre O, Aly M, Björklund J, Olsson M, Adding C, u. a. Preoperative staging using magnetic resonance imaging and risk of positive surgical margins after prostate-cancer surgery. Prostate Cancer Prostatic Dis. September 2019;22(3):391–8.
11. McEvoy SH, Raeside MC, Chaim J, Ehdaie B, Akin O. Preoperative Prostate MRI: A Road Map for Surgery. Am J Roentgenol. August 2018;211(2):383–91.
12. Quentin M, Schimmöller L, Ullrich T, Valentin B, Demetrescu D, Al-Monajjed R, u. a. Pre-operative magnetic resonance imaging can predict prostate cancer with risk for positive surgical margins. Abdom Radiol. Juli 2022;47(7):2486–93.
13. Veerman H. The detection rate of apical tumour involvement on preoperative MRI and its impact on clinical outcomes in patients with localized prostate cancer. J Robot Surg. 2022;
14. Xu L, Zhang G, Zhang D, Zhang J, Zhang X, Bai X, u. a. An MRI-based grading system for preoperative risk estimation of positive surgical margin after radical prostatectomy. Insights Imaging. 23. Oktober 2023;14(1):178.
15. Halis A, Gelmis M, Caglar U, Hacibey I, Sekkeli S, Yazılı HB, u. a. Association of surgical margin positivity with preoperative mpMRI-identified index lesions in radical prostatectomy: A retrospective study. Can Urol Assoc J [Internet]. 16. Mai 2025 [zitiert 30. Dezember 2025];19(9). Verfügbar unter: https://cuaj.ca/index.php/journal/article/view/9103
16. Chen X, Chen Y, Qian C, Wang C, Lin Y, Huang Y, u. a. Multiparametric MRI lesion dimension as a significant predictor of positive surgical margins following laparoscopic radical prostatectomy for transitional zone prostate cancer. World J Urol. 12. Mai 2025;43(1):295.
17. Rosenkrantz AB, Shanbhogue AK, Wang A, Kong MX, Babb JS, Taneja SS. Length of capsular contact for diagnosing extraprostatic extension on prostate MRI: Assessment at an optimal threshold: Diagnosing EPE on Prostate MRI. J Magn Reson Imaging. April 2016;43(4):990–7.

18. Mehralivand S, Shih JH, Harmon S, Smith C, Bloom J, Czarniecki M, u. a. A Grading System for the Assessment of Risk of Extraprostatic Extension of Prostate Cancer at Multiparametric MRI. Radiology. März 2019;290(3):709–19.
19. Alessi S, Maggioni R, Luzzago S, Colombo A, Pricolo P, Summers PE, u. a. Apparent Diffusion Coefficient and Other Preoperative Magnetic Resonance Imaging Features for the Prediction of Positive Surgical Margins in Prostate Cancer Patients Undergoing Radical Prostatectomy. Clin Genitourin Cancer. Dezember 2021;19(6):e335–45.
20. Yao A, Iwamoto H, Masago T, Morizane S, Honda M, Sejima T, u. a. The Role of Staging MRI in Predicting Apical Margin Positivity for Robot-Assisted Laparoscopic Radical Prostatectomy. Urol Int. 2014;93(2):182–8.
21. Soeterik TFW, Van Melick HHE, Dijksman LM, Stomps S, Witjes JA, Van Basten JPA. Nerve Sparing during Robot-Assisted Radical Prostatectomy Increases the Risk of Ipsilateral Positive Surgical Margins. J Urol. Juli 2020;204(1):91–5.
22. Yossepowitch O, Briganti A, Eastham JA, Epstein J, Graefen M, Montironi R, u. a. Positive Surgical Margins After Radical Prostatectomy: A Systematic Review and Contemporary Update. Eur Urol. Februar 2014;65(2):303–13.
23. Van Der Slot MA, Remmers S, Kweldam CF, Den Bakker MA, Nieboer D, Busstra MB, u. a. Biopsy prostate cancer perineural invasion and tumour load are associated with positive posterolateral margins at radical prostatectomy: implications for planning of nerve-sparing surgery. Histopathology. September 2023;83(3):348–56.
24. Cozzi G, Rocco BM, Grasso A, Rosso M, Abed El Rahman D, Oliva I, u. a. Perineural invasion as a predictor of extraprostatic extension of prostate cancer: A systematic review and meta-analysis. Scand J Urol. Dezember 2013;47(6):443–8.

Figure legends

Figure 1. a. axial DWI with calculated b=2000. b. axial T2-weighted image. c. axial ADC map. d. axial DCE imaging with subtraction during arterial phase. 80-year-old patient with PI-RADS 4 lesion at the mid level of the prostate in the posteromedial and posterolateral peripheral zone (white arrows) with suspicion of extraprostatic extension (white arrow heads). Postoperative histopathological examination proved R1 resection.

Figure 2. a. axial DWI with calculated b=2000. b. axial ADC map. c. axial DCE imaging with subtraction during arterial phase. d. axial T2-weighted image. 73-year-old patient with PI-RADS 5 lesion at the mid level of the prostate (white arrows) without capsular contact or urethral involvement (white arrow heads). Postoperative histopathological examination proved R0 resection.

Figure 3. a. coronal T2-weighted image. b. axial T2-weighted image. c. axial DWI with calculated b=2000. d. axial ADC map. 67-year-old patient with PI-RADS 5 lesion at the prostate base with broad capsular contact (white arrows), seminal vesicle infiltration and

extraprostatic extension and urethral involvement (white arrow heads). Postoperative histopathological examination proved R1 resection.

Figure 4. a. axial T2-weighted image. b. axial DWI with calculated b=2000. c. axial DCE imaging with subtraction during arterial phase. d. axial ADC map. 75-year-old patient with PI-RADS 5 lesion at the mid level of the prostate with large diameter (34 mm) and broad capsular contact (white arrows) and urethral involvement (white arrow head). Postoperative histopathological examination proved R1 resection.

Figure 5. a. axial T2-weitghted image. b. axial DWI with calculated b=2000. c. coronal T2-weighted image. d. axial ADC map. 75-year-old patient with middle prostate PI-RADS 4 lesion at the posterolateral and anterior peripheral zone border with short capsular contact (white arrows). No evidence of seminal vesicle infiltration, extraprostatic extension or urethral involvement (white arrow heads). Postoperative histopathological examination proved R0 resection.

Figure 6. a. axial T2-weighted image. b. axial DWI with calculated b=2000. c. axial DCE imaging with subtraction during arterial phase. d. coronal T2-weighted image. 62-year-old patient with a PI-RADS 4 lesion at the prostate base (white arrow) with suspicion of seminal vesicle infiltration (white arrow head). Postoperative histopathological examination showed positive resection margins.

Table 1A. Patient characteristics according to surgical margin status in 134 patients undergoing robot-assisted radical prostatectomy. Clinical, histopathological, and surgical parameters according to surgical margin status

(n= 134)	Negative surgical margins n= 107	Positive surgical margins n= 27	p-value
Clinical parameters			
Age (years)	66.1 ± 7.0	65.9 ± 6.8	0.796*
BMI	27.0 ± 3.7	27.6 ± 4.6	0.833*
PSA (ng/ml)	8.85 ± 6.67	32.52 ± 78.90	**< 0.001***
Prostate volume (cm^3)	91.6 ± 47.8	87.2 ± 45.3	0.767*
PSA density (ng/ml^2)	0.11 ± 0.09	0.33 ± 0.54	**< 0.001***
PSA density >0.15 (ng/ml^2)	24% (n=26)	59% (n=16)	**<0.001****
Histopathological parameters			
Positive biopsy cores (%)	34.7 ± 20.0	43.7 ± 22.3	**0.029***
ISUP group in biopsy	2.4 ± 1.2	2.4 ± 1.0	0.779*
ISUP group in prostate specimen	2.4 ± 0.9	2.4 ± 0.6	0.35*
Infiltration of perineural sheath (prostate specimen)	70% (n= 76)	96% (n= 26)	**0.01****
Extraprostatic extension (prostate specimen)	28% (n= 30)	48% (n= 13)	**0.037****
Surgical parameters			
RARP duration (h)	2.87 ± 0.66	3.14 ± 0.57	**0.046***
Days between MRI and RARP	136.0 ± 69.5	114.2 ± 64.1	0.158*
Nerve sparing surgery	62% (n= 66)	52% (n= 14)	0.385**

Table 1B. MRI-Derived characteristics according to surgical margin status

(n= 134)	Negative surgical margins n= 107	Positive surgical margins n= 27	p-value
Number of PI-RADS lesions	1.51 ± 0.65	1.33 ± 0.48	0.250*
Highest PI-RADS Score	4.2 ± 0.4	4.4 ± 0.7	0.054*
Presence of PI-RADS 5 lesion	24% (n= 26)	44% (n= 12)	0.055*
Sum of PI-RADS diameters	16.6 ± 8.1	24.4 ± 16.8	**0.027***
Lesion density (mm/ cm^3)	0.22 ± 0.15	0.35 ± 0.28	**0.024***
Multifocality	89% (n= 95)	100% (n= 27)	0.124**
Presence of a lesion with capsular contact	65% (n= 69)	93% (n= 25)	**0.004**
Presence of a lesion with > 12mm length of capsular contact	16% (n=17)	63% (n=17)	**< 0.001**
Extra-prostatic extension	7% (n= 7)	59% (n= 16)	**< 0.001****
Seminal vesicle infiltration	4% (n= 4)	15% (n= 4)	**0.046****
Urethral involvement (distance < 2mm)	9% (n=10)	41% (n=11)	**< 0.001**
Apical involvement	70% (n= 75)	78% (n=21)	0.484
Lymph node involvement	4% (n= 4)	11% (n= 3)	0.145**

Note: Values are presented as mean ± standard deviation or percentage (number of patients), as appropriate.
* Statistical significance assessed using Mann-Whitney U- test for continuous variables.
**Chi-squared test or Fisher's exact test used for categorical variables.

Abbreviations:
BMI = Body Mass Index; PSA = Prostate-Specific Antigen; ISUP = International Society of Urological Pathology; RARP = Robot-Assisted Laparoscopic Prostatectomy; PI-RADS = Prostate Imaging Reporting and Data System; MRI = Magnetic Resonance Imaging; mm = millimeters; cm^3 = cubic centimeters.

Table 2. Lesion characteristics stratified by patient surgical margin status (n = 202 Lesions)

(n= 202)	Lesions from patients with negative surgical margins n=162	Lesions from patients with positive surgical margins n=40	p-value
Length of capsular contact (mm)	5.5 ± 5.8	13.2 ± 10.8	**< 0.001***
PI-RADS volume (cm^3)	0.54 ± 0.68	2.12 ± 3.74	**0.014***
PI-RADS	4.1 ±0.5	4.4 ± 0.5	**0.005***
PI-RADS ADC	430 ± 143	428 ± 138	0.874*
PI-RADS urethral distance (mm)	9.3 ± 5.4	7.3 ± 6.5	**0.02***
PI-RADS max. diameter (mm)	11.0 ± 4.9	16.5 ± 10.5	**0.005***
Presence of capsular contact	60% (n= 97)	85% (n= 34)	**0.003****
Lesion in apical third of the prostate	42% (n= 68)	38% (n= 15)	0.720**
Arterial hyperperfusion	46% (n= 75)	83% (n= 33)	**< 0.001****
Suspicion of extra-prostatic extension	5% (n= 8)	50% (n= 20)	**< 0.001****

Note: Values are presented as mean ± standard deviation or percentage (number of lesions), as appropriate. Lesions were stratified according to the surgical margin status of the corresponding patient. Surgical margin status was determined at the patient level and was not assigned to individual lesion locations.

Abbreviations:
PI-RADS = Prostate Imaging Reporting and Data System;
ADC = Apparent Diffusion Coefficient;
MRI = Magnetic Resonance Imaging;
mm = millimeters; cm^3 = cubic centimeters.

Table 3. Univariate logistic regression analysis of clinical, histopathological, surgical, and MRI-derived parameters for predicting resection margin status

	OR	95%CI	p-value
Clinical parameters			
PSA (ng/ml)	**1.06**	1.02 – 1.11	**0.006**
PSA density (ng/ml^2)	**6.61**	1.92 – 23.10	**< 0.001**
PSA density >0.15 (ng/ml^2)	**4.53**	1.87 – 10.99	**<0.001**
Histopathological parameters in biopsy			
Percentage of positive specimen (%)	**1.02**	1.00 – 1.04	**0.048**
Infiltration of perineural sheath	**10.61**	1.38 – 81.6	**0.023**
Surgical parameter			
RARP duration (h)	**1.93**	0.98 – 3.78	**0.046**
MRI parameters			
Sum of PI-RADS diameters	**1.06**	1.02 – 1.11	**0.04**
Lesion density (mm/ cm^3)	**19.05**	2.26 – 160.58	**0.007**
Presence of a lesion with capsular contact	**6.88**	1.55 – 30.66	**0.011**
Presence of a lesion with > 12mm length of capsular contact	**9.00**	3.53 – 22.98	**< 0.001**
Extra-prostatic extension	**21.04**	7.27 – 60.88	**< 0.001**
Seminal vesicle infiltration	**4.48**	1.04 – 19.24	**0.044**
Urethral involvement (distance < 2mm)	**6.67**	2.44 – 18.25	**< 0.001**

Note: Odds ratios (OR) with 95% confidence intervals (CI) and p-values are presented for each clinical, histopathological, surgical and MRI-derived variable. Statistical significance was determined using univariate logistic regression analysis. A p-value of < 0.05 was considered statistically significant.

Abbreviations:
PSA = Prostate-Specific Antigen;
RARP = Robot-Assisted Laparoscopic Prostatectomy;
PI-RADS = Prostate Imaging Reporting and Data System;
MRI = Magnetic Resonance Imaging;
mm = millimeters; cm^3 = cubic centimeters;
EPE = Extra-Prostatic Extension.

Figure 1

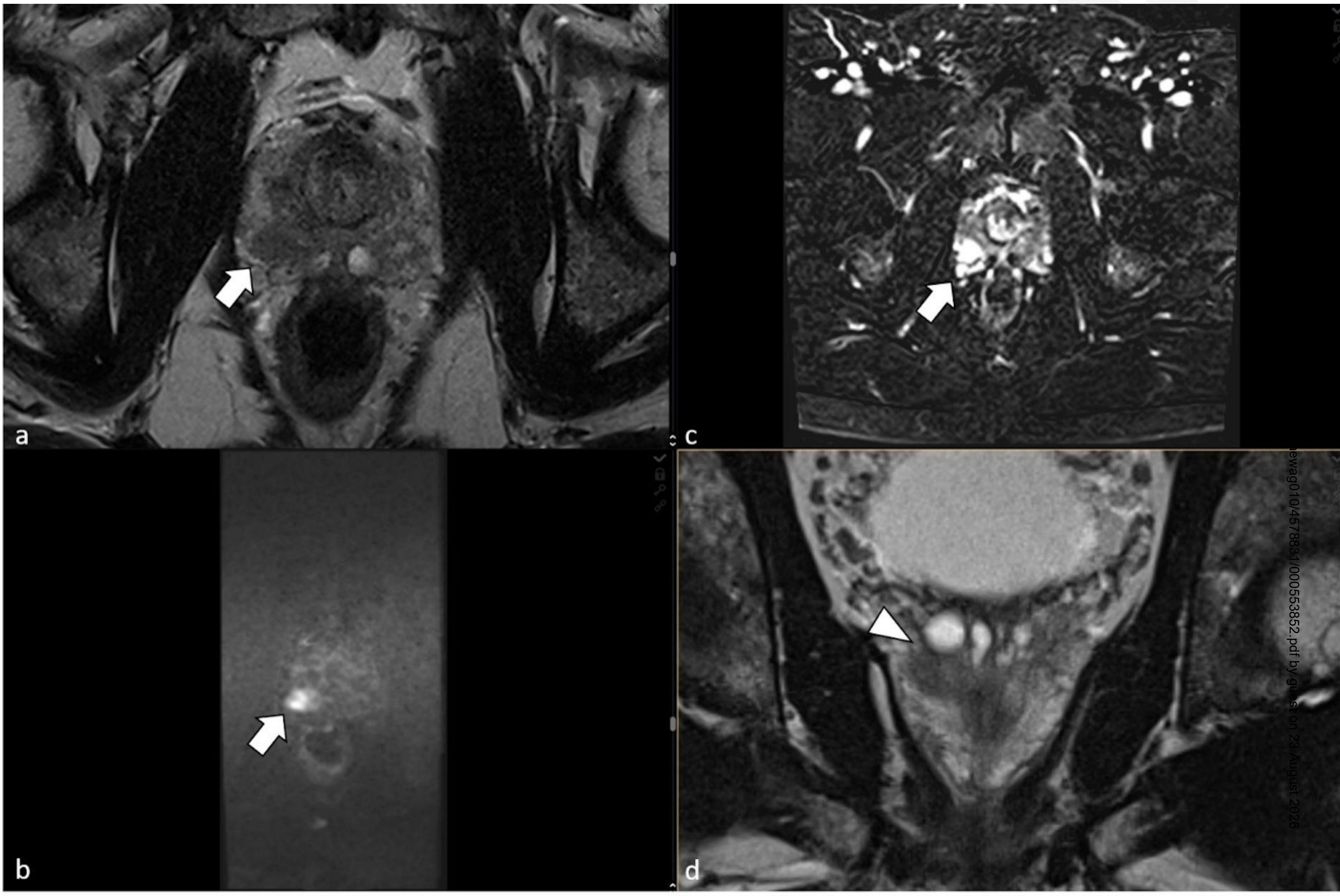

Figure 2

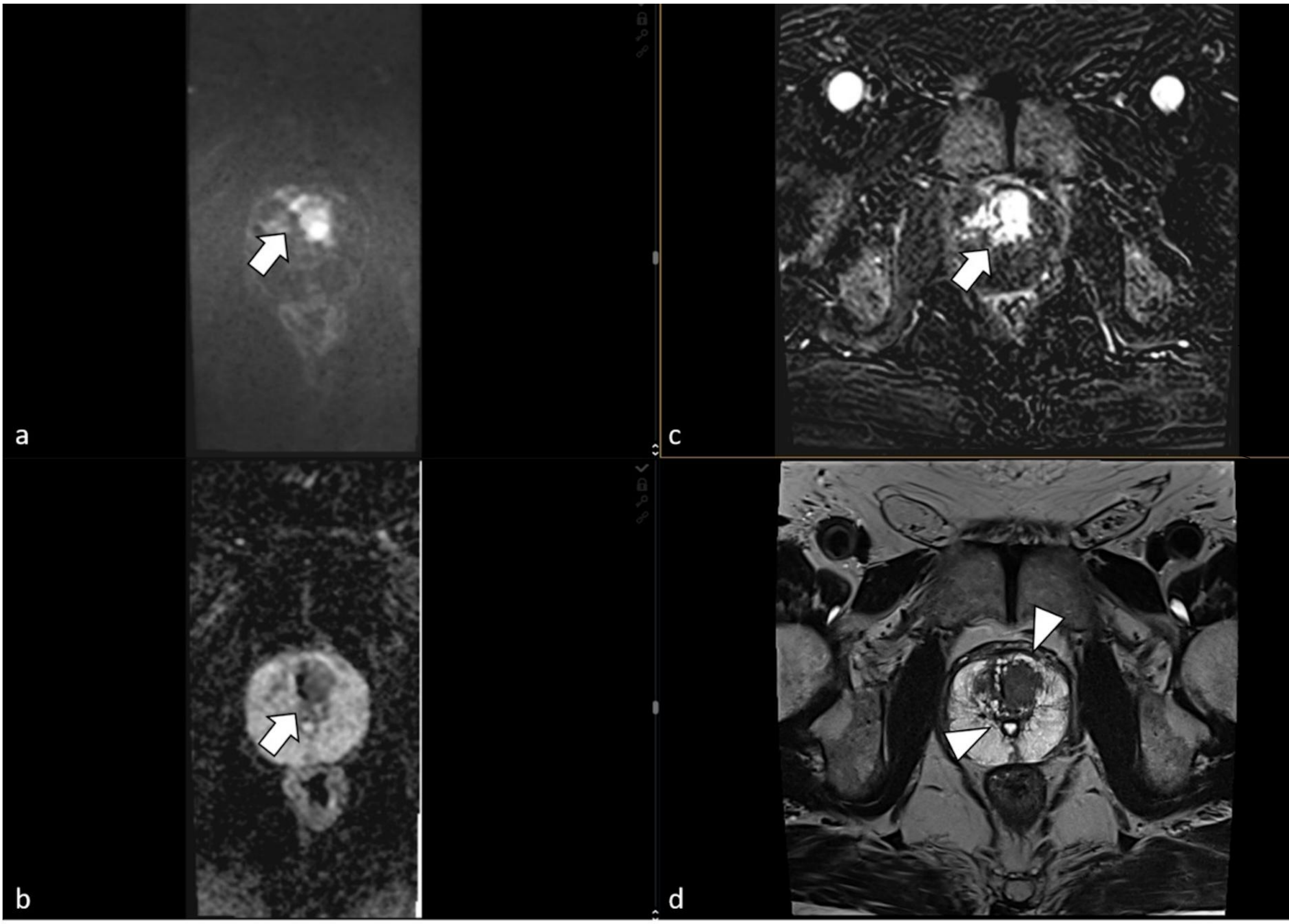

Figure 3

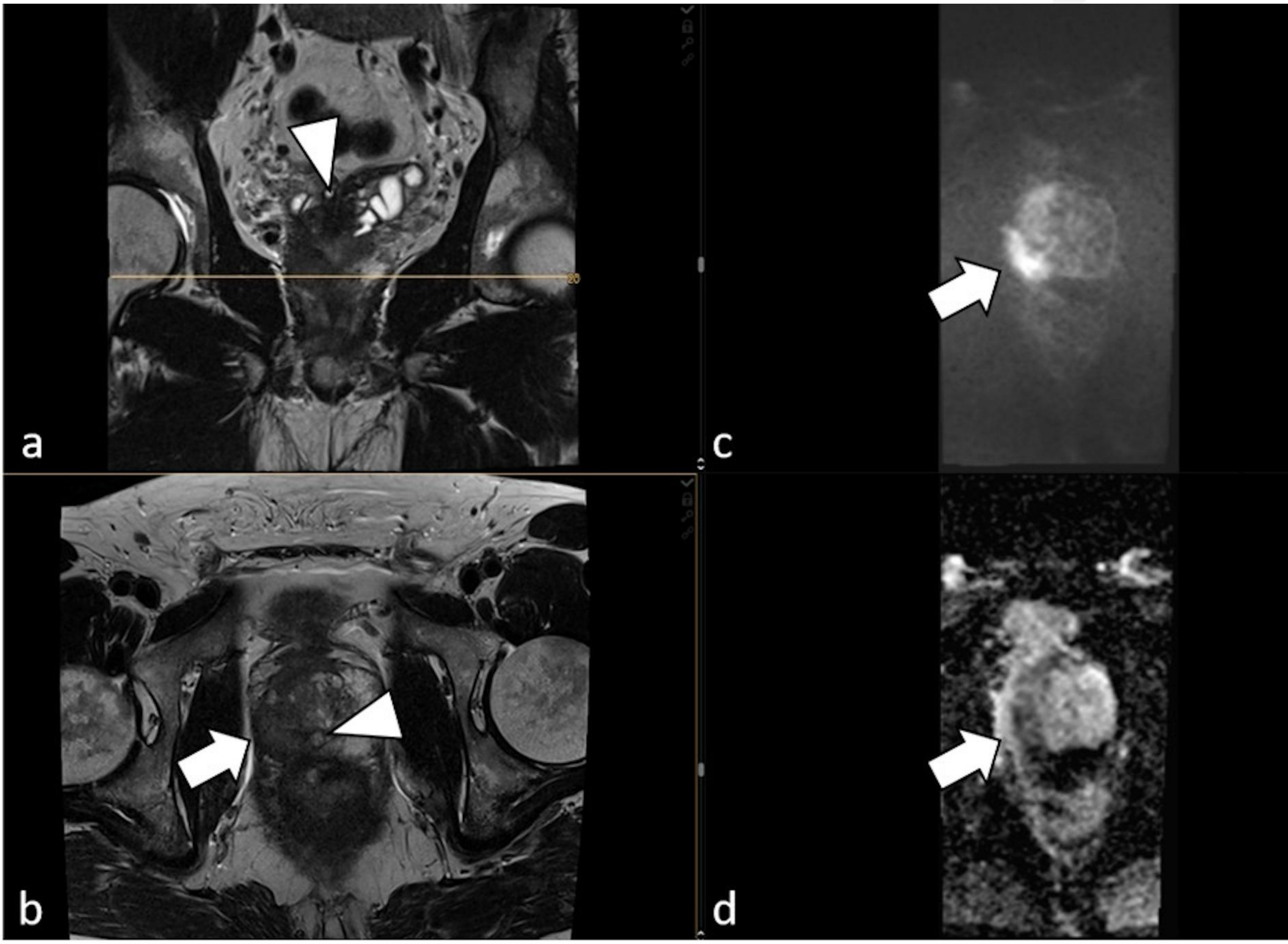

Figure 4

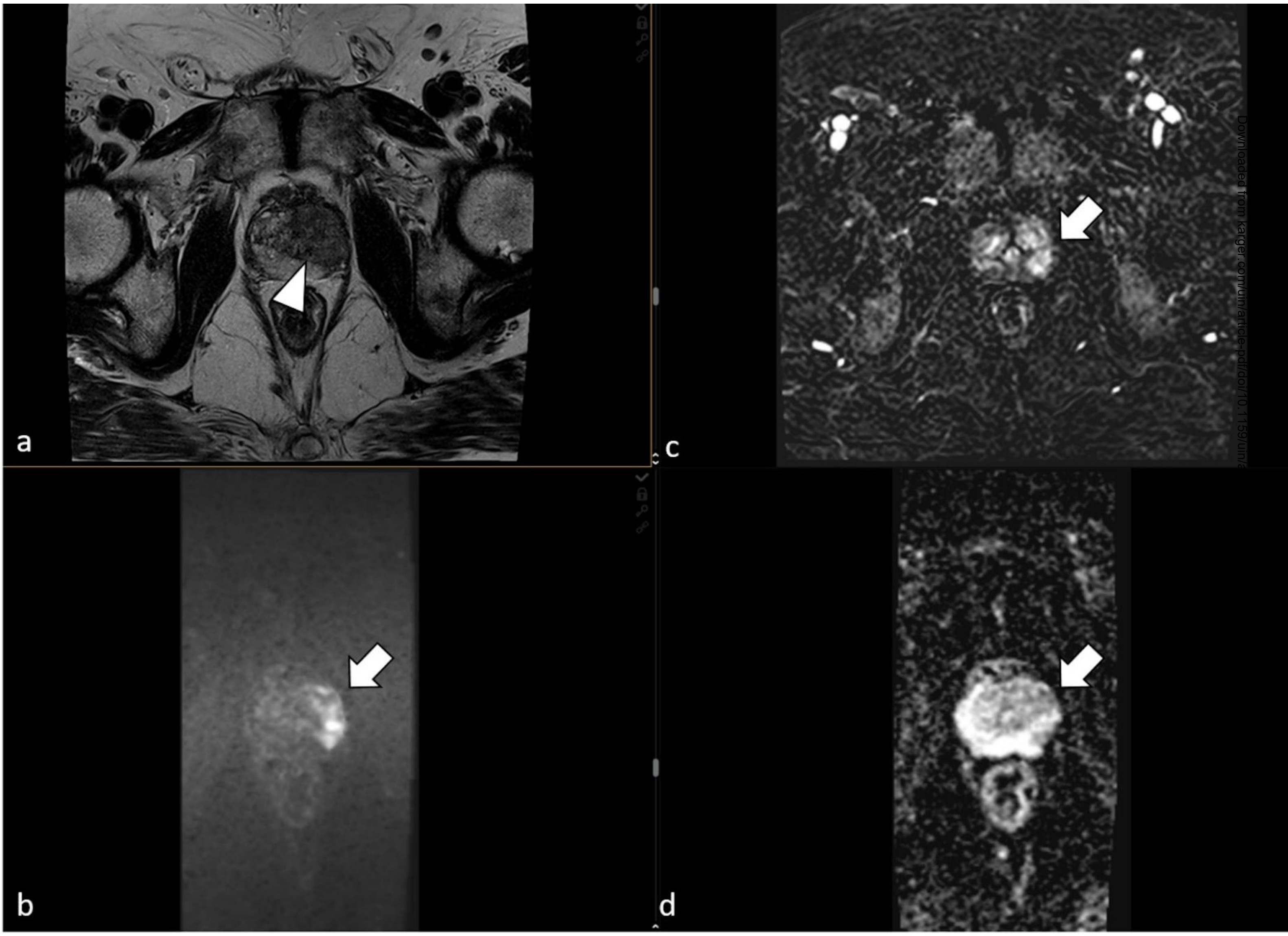

Figure 5

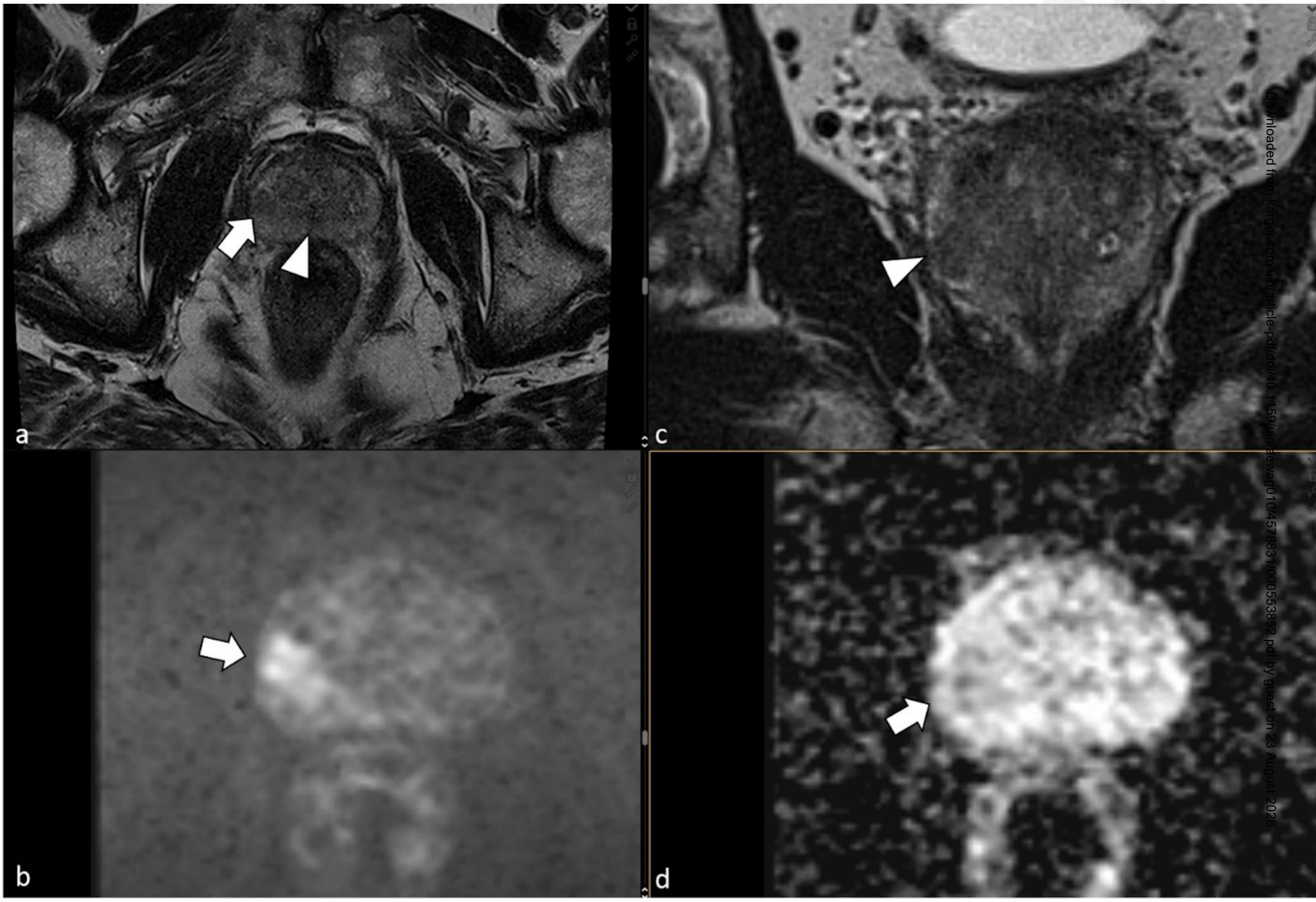

Figure 6